PHOTONICS Research

Continuous wave operation of GaAsBi microdisk lasers at room temperature with large wavelengths ranging from 1.27 to 1.41 μm

Xiu Liu,[1,†] Lijuan Wang,[2,3,†] Xuan Fang,[1,4,†] Taojie Zhou,[1] Guohong Xiang,[1] Boyuan Xiang,[1] Xueqing Chen,[1] Suikong Hark,[1] Hao Liang,[2,3] Shumin Wang,[2,5,6] and Zhaoyu Zhang[1,7]

[1]School of Science and Engineering, The Chinese University of Hong Kong, Shenzhen 518172, China
[2]University of Chinese Academy of Sciences, Beijing 100049, China
[3]Key Laboratory of Terahertz Solid-State Technology, Chinese Academy of Sciences, Shanghai Institute of Microsystem and Information Technology, CAS, Shanghai 200050, China
[4]Key Laboratory for Photonic and Electronic Bandgap Materials, Ministry of Education, School of Physics and Electronic Engineering, Harbin Normal University, Harbin 150025, China
[5]Department of Microtechnology and Nanoscience, Chalmers University of Technology, 41296 Gothenburg, Sweden
[6]e-mail: shumin@mail.sim.ac.cn
[7]e-mail: zhangzy@cuhk.edu.cn

Received 6 December 2018; revised 22 February 2019; accepted 5 March 2019; posted 5 March 2019 (Doc. ID 354686); published 12 April 2019

Submicron-meter size GaAsBi disk resonators were fabricated with the GaAsBi/GaAs single-quantum-well (QW)-structure grown by molecular beam epitaxy. The GaAsBi/GaAs QW revealed very broad photoluminescence signals in the wavelength range of 1100–1400 nm at 300 K. The 750 nm diameter and 220 nm thick disk resonators were optically pumped and exhibited lasing characteristics with continuous wave operation at room temperature. To our knowledge, it is the first demonstration of a lasing wavelength longer than 1.3 μm with a maximum value of 1.4 μm in a GaAsBi/GaAs material system. The lasing wavelength spans about 130 nm by adjusting the disk diameter, covering almost the entire O band. The ultrasmall GaAsBi disk lasers may have great potential for highly dense on-chip integration with large tunability in the O band.

https://doi.org/10.1364/PRJ.7.000508

1. INTRODUCTION

GaAsBi with its novel properties is a promising candidate to address the limitations of the conventional material for telecommunication semiconductor lasers [1–5]. Compared to In and Sb, incorporating Bi into GaAs leads to a faster decrement in the bandgap of GaAs and broader luminescence spectral width [6], resulting in a great flexibility of wavelength extension and tunability for telecommunication with only a small change in lattice constant [7]. It is also less detrimental in terms of optical quality as compared to GaAsN [8,9]. In addition, alloying Bi in GaAs enlarges spin–orbit (SO) split-off energy. When the SO split-off energy is larger than the bandgap of GaAsBi, the detrimental effects of Auger recombination and intervalence band absorption can be drastically mitigated or even eliminated, thus significantly enhancing the thermal stability and characteristic temperature of GaAsBi quantum well (QW) lasers [7,10,11]. Other beneficial properties include less temperature-sensitive bandgaps, minor influence on both electron and hole mobility for small Bi concentrations, enhancement of photoluminescence (PL) intensity and surfactant effect ensuring smooth surface, etc. [12]. Based on these attractive properties, GaAsBi has been widely studied in recent years for promises in the applications of wavelength-tunable light sources [13,14], integration with silicon photonics [15,16], and high-speed modulation [17,18]. However, large incorporation of Bi with decent optical quality is technically challenging because of the strong tendency of Bi to segregate toward the surface and the used low-growth temperatures, which degrades the optical quality [19]. This limits the lasing wavelength extension, and introducing nanocavities tends to help fill the large gap to 1.3 μm and even 1.55 μm to enable wide-range tuning of its resonance frequency [20,21].

As one of the excellent candidates for on-chip high-speed applications, a whispering-gallery-mode (WGM) microdisk cavity with an ultrahigh quality factor and a small mode volume can be applied in Raman sources [19], ultralow threshold lasers, nanoparticle detection [20,21], and temperature or micromechanical vibration sensors [22,23]. Submicron microdisk lasers exhibit large-mode spacing, and single-mode lasing can also be obtained [24]. In addition, the lasing spectra and mode behaviors of WGMs are highly sensitive to the environmental changes such as structural deformation [25] and changes in

the temperature or refractive index of the surrounding medium [26,27]. More importantly, the ultrasmall disk laser with a small footprint has great potential in modern photonic integration compared to Fabry–Perot (FP)-based GaAsBi lasers. GaAsBi lasers with an FP cavity have been extensively reported with up-to-date 5.80% Bi composition and electrically pumped lasing at 1.142 μm by Wang's group [28]. However, no GaAsBi disk laser at nanoscale has ever been reported.

In this work, we report, to the best of our knowledge, the first demonstration of GaAsBi microdisk lasers with a low threshold emitting in the telecommunication wavelength range. The lasers are optically pumped in continuous wave (CW) mode and operated at room temperature. The single $GaAs_{1-x}Bi_x$ QW lasers with $x = 5.8\%$ exhibit single-mode lasing with a large tunability over 130 nm by geometry engineering, achieving a maximum lasing wavelength up to 1407 nm.

2. DEVICE FABRICATION

A GaAs/GaAsBi single-QW laser structure was grown by DCA P600 solid-source molecular beam epitaxy (MBE) on n-doped GaAs (001) substrates. The schematic diagram of the QW structure can be seen in Fig. 1(a). The laser structure contains three parts: 100 nm thick GaAs buffer layer, 1 μm $Al_{0.95}Ga_{0.05}As$, and 220 nm active layer including a single $GaAs/GaAs_{0.942}Bi_{0.058}$ QW. Other detailed growth conditions were described in the previous work [22]. After epitaxial growth, the sample was transferred into a rapid thermal annealing (RTA) system with the annealing temperature kept at 500°C for 30 s. The annealing procedure was carried out under a nitrogen atmosphere using a commercial RTA reactor (AccuThermo AW410, Allwin21 Corp.).

Cross-sectional transmission electron microscopy (TEM) images of as-grown and annealed samples are shown in Figs. 1(b) and 1(c), respectively. For the as-grown sample, the dark area is a GaAsBi QW layer with a thickness about 15 nm marked by yellow dashed lines, and the surrounding bright areas are GaAs barrier layers. Nonuniform contrast within and around the QW with a typical nanoscale size of 10 nm marked by the red circle can be seen clearly, indicating inhomogeneous local strain fluctuation and/or Bi distribution. After RTA treatment, a rearrangement of Bi atoms and clusters inside the GaAsBi QW could be realized, similar to the cases for other group-V elements [23–25]. As a result, a clear interface and uniform GaAsBi QW can be obtained, as shown in Fig. 1(c).

The microdisk patterns were defined by electron beam lithography with Zep520 (120 nm via 3600 rounds/s spin coating) acting as an electron beam resist, and the mask pattern was

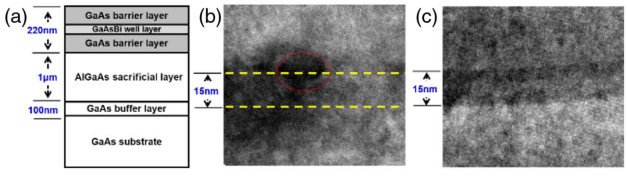

Fig. 1. (a) Schematic diagram of the GaAsBi/GaAs single QW structure. (b) TEM image showing the as-grown 15 nm thick single GaAsBi/GaAs QW. (c) TEM image showing the same QW after RTA.

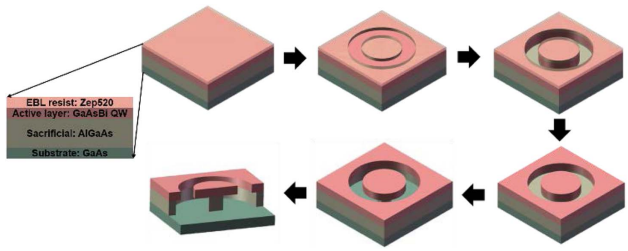

Fig. 2. Fabrication process of the GaAsBi microdisk. The electron beam lithography resist Zep520 is directly spin-coated on the wafer, with subsequent inductively coupled plasma-reactive ion etching transferring the disk pattern down to the active layer. Finally, the AlGaAs sacrificial layer is oxidized and then undercut by hydrofluoric acid for the free-standing disk.

transferred through the GaAsBi/GaAs single QW with inductively coupled plasma-reactive ion etching [26]. Compared to our previous works [27,28], no hard mask is used, which greatly simplifies the process while keeping an excellent disk topology at the nanoscale with small surface roughness. The supporting AlGaAs posts were formed by selective wet etching (with dilute hydrofluoric acid for 10 s, then 30 s for IPA and deionized water, respectively), resulting in a free-standing microdisk for increased optical confinement. The detailed fabrication flow chart is shown in Fig. 2. Then the fabricated microdisks were characterized in a microscopic photoluminescence system at room temperature under CW optical pumping using a 632.8 nm He–Ne laser with a spot size around 2 μm. The pumping power is used as absorbed power after considering the effective pumping area and surface reflection.

3. DEVICE CHARACTERIZATION

Apparent peaks are shown on the PL spectra of the GaAsBi microdisk laser with a radius of 0.75 μm covering 1100–1400 nm in Fig. 3. Finite-difference time-domain (FDTD) simulations were carried out. We chose a simple cylinder geometry with a height of 220 nm [thickness of the QW layer shown

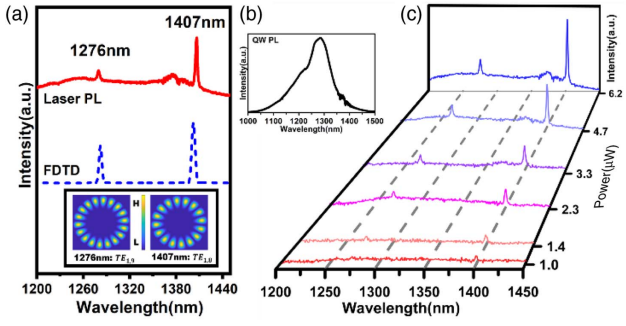

Fig. 3. (a) Cold disk cavity oscillates with the gain QW structure resulting in the lasing behavior with a good consistency of FSR between theoretical and experimental (pumping of 101.2 μW) results. The inset is the FDTD simulation for mode profiles of lasing wavelengths 1276 nm and 1407 nm, respectively. (b) GaAsBi QW PL well covers the wavelength range from 1100 to 1400 nm. (c) The evolution of PL spectra of the GaAsBi microdisk laser of radius 0.75 μm at various pumping power.

in Fig. 1(a)], and a refractive index of 3.6 [29]. The lasing optical modes are shown in Fig. 3(a), indicating the lasing peaks at 1276 nm and 1407 nm are the $TE_{1,9}$ and $TE_{1,8}$ modes, respectively. Since the disk is undercut from the periphery for enhanced optical confinement, high radial-order WGMs are concentrated spatially close to the disk center and leak through the AlGaAs pedestal, and only the lowest order WGMs can be sustained and oscillate around the disk edges. The free-spectral-range (FSR) modes with successive angular mode numbers can be calculated by $\Delta\lambda_{FSR} \approx \frac{\lambda^2}{2\pi \cdot R \cdot n}$, where R is the disk radius and n is the effective refractive index. The theoretical result of FSR = 124 nm agrees well with our experimental result, which is 131 nm. The deviation between the FDTD simulation and PL result can be explained in two parts: one is the imperfectness of fabrication in which the disk edge roughness and slope can significantly influence the mode distribution; the other is the uncertainty in the refractive index of the nonuniformly distributed Bi of GaAsBi QW layer.

The GaAsBi QW (no pattern) PL is shown in Fig. 3(b) and well covers the wavelength from 1100 to 1400 nm. After coupling with the cold cavity modes, lasing behaviors are expected [30–32]. The collected PL spectra under various CW pumping power are shown in Fig. 3(c). At a low pumping power of 15.8 μW, only spontaneous emission is apparent. As the power increases, sharp lasing peaks located at 1276 nm and 1407 nm arise, which are obvious evidence of lasing.

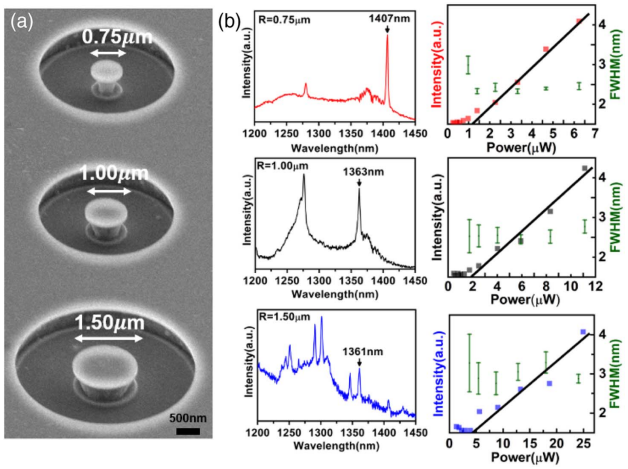

Fig. 4. (a) Scanning electron microscopy images of a fabricated GaAsBi microdisk laser at different radii. (b) The collected PL spectra for the GaAsBi microdisk laser with a radius of 0.75, 1.00, and 1.50 μm with related L–L curves and FWHMs. The chosen peak is indicated by a black arrow. For the smallest radius of 0.75 μm, the lasing threshold is 1.2 μW and the FWHM is 2.5 ± 0.3 nm.

Scanning electron microscopy images of a fabricated GaAsBi microdisk laser at radii of 0.75 μm, 1.00 μm, and 1.50 μm with an excellent topology are shown in Fig. 4(a). The output signal intensity tends to decrease with increasing radius of the microdisk (as shown in supporting information). Further PL details are given in Fig. 4(b) presenting the collected PL spectra and the corresponding light in–light out (L–L) curves of the disks with different radii. For the disk with a radius of 0.75 μm, the L–L curve for the lasing peak at 1407 nm is shown with a pronounced kink point of the threshold extrapolated to be 1.2 μW. The related full width at half-maximum (FWHM) of the emission spectra also changes simultaneously with the pumping power, indicating a clear laser threshold, and the FWHM above the threshold of the 1407 nm lasing peak is 2.5 ± 0.3 nm.

The same analysis has been taken for a disk with a radius at 1.00 μm with a peak of 1363 nm and 1.50 μm with a peak of 1361 nm. The lasing thresholds for the radius of 1.00 μm and 1.50 μm are 1.8 μW and 3.3 μW, respectively. The FWHM of the two radii also changes simultaneously with a value of 2.6 ± 0.6 nm for 1.00 μm and 3.0 ± 0.9 nm for 1.50 μm at the above threshold conditions. With different radii, the lasing wavelengths well cover the range from 1.27 to 1.4 μm. This broad lasing tunability based on disk geometry provides a possibility for next-generation on-chip tunable coherent light source.

To better understand the advantages of our GaAsBi microdisk laser, Table 1 summarizes the up-to-date GaAsBi laser performance. We introduced the microdisk cavity based on a GaAsBi QW structure with a Bi concentration as high as 5.8% for improved gain medium and optical mode coupling for the first time, to the best of our knowledge, in this work. Compared to precious FP-based lasers, we successfully extend lasing wavelength to the telecommunication range by changing the disk radius, which gives great potential for laser wavelength tuning. Combining other properties of the microdisk cavity including a small footprint, a high Q-factor, and WGM-based high sensitivity with the beneficial properties of GaAsBi materials, including large bandgap bowing and excellent thermal stability, the GaAsBi microdisk laser plays an important role for a cooler-free high-speed silicon-integrated circuit enabling a path to next-generation telecom technology.

4. CONCLUSION

In this paper, we have fabricated a GaAsBi microdisk laser based on QW structure with a Bi concentration of 5.8%. The lasing

Table 1. Brief Summary of GaAsBi-Based Infrared Lasers

Year	Structure	Bi Concentration (%)	Pumping	Cavity	Lasing Wavelength (nm)	Reference
2010	Bulk	2.5	OP-pulsed	FP	982.8, 986.2	[33]
2013	Bulk	4.2	OP-pulsed	FP	1088.6, 1204	[34]
2013	QW	2.2	EP-pulsed	FP	947	[35]
2014	QW	6	EP-pulsed	FP	1060	[36]
2014	Bulk	3, 4	EP-pulsed	FP	976, 1045	[37]
2017	QW	5.8	EP-pulsed & CW	FP	1142, 1135	[28,38]
2018	QW	5.8	OP-CW	Microdisk	1276, 1407	This work

behaviors are observed at different radii with the smallest one of 0.75 μm with lasing wavelengths at 1276 nm and 1407 nm well covering the telecom range. The microdisk cavity at nanoscale also results in a low threshold of 21 ± 5 μW and a narrow FWHM of 2.6 ± 0.5 nm. The lasing wavelength can be tuned by varying the microdisk radius, providing great potential for the GaAsBi-based tunable lasers. Together with the advantages of a microdisk cavity, GaAsBi QW lasers can be of significance for compact and high-speed photonic integration on the Si platform.

Funding. Shenzhen Key Laboratory Project Grant (ZDSYS201603311644527); Shenzhen Fundamental Research Fund (JCYJ20150611092848134, JCYJ20150929170644623); Shenzhen Science and Technology Innovation Commission (KQCX20140522143114399); President's Fund (PF01000154); Foundation NANO X (18JG01); National Natural Science Foundation of China (NSFC) (11474365, 61334004, 61404152); National Basic Research Program of China (973 Project) (2014CB643902); Vetenskapsrådet (VR); Robotic Discipline Development Fund from Shenzhen Gov. (2016-1418); Open Project Program of Key Laboratory for Photonic and Electric Bandgap Materials, Ministry of Education, Harbin Normal University, China (PEBM201902).

†These authors contributed equally to this work.

REFERENCES

1. L. A. Coldren, "Monolithic tunable diode lasers," IEEE J. Sel. Top. Quantum Electron. **6**, 988–999 (2000).
2. C. F. Lin, Y. S. Su, and B. R. Wu, "External-cavity semiconductor laser tunable from 1.3 to 1.54 μm for optical communication," IEEE Photon. Technol. Lett. **14**, 3–5 (2002).
3. S. Mokkapati and C. Jagadish, "III-V compound SC for optoelectronic devices," Mater. Today **12**, 22–32 (2009).
4. R. Wang, S. Sprengel, A. Vasiliev, G. Boehm, J. Van Campenhout, G. Lepage, P. Verheyen, R. Baets, M.-C. Amann, and G. Roelkens, "Widely tunable 23 μm III-V-on-silicon Vernier lasers for broadband spectroscopic sensing," Photon. Res. **6**, 858–866 (2018).
5. N. Zhang, X. Cai, and S. Yu, "Optical generation of tunable and narrow linewidth radio frequency signal based on mutual locking between integrated semiconductor lasers," Photon. Res. **2**, B11–B17 (2014).
6. S. Tixier, M. Adamcyk, T. Tiedje, S. Francoeur, A. Mascarenhas, P. Wei, and F. Schiettekatte, "Molecular beam epitaxy growth of $GaAs_{1-x}Bi_x$," Appl. Phys. Lett. **82**, 2245–2247 (2003).
7. K. K. Nagaraja, Y. A. Mityagin, M. P. Telenkov, and I. P. Kazakov, "$GaAs_{(1-x)}Bi_x$: a promising material for optoelectronics applications," Crit. Rev. Solid State Mater. Sci. **42**, 239–265 (2017).
8. D. L. Young, J. F. Geisz, and T. J. Coutts, "Nitrogen-induced decrease of the electron effective mass in $GaAs_{1-x}N_x$ thin films measured by thermomagnetic transport phenomena," Appl. Phys. Lett. **82**, 1236–1238 (2003).
9. S. M. Wang, G. Adolfsson, H. Zhao, Y. Q. Wei, J. Gustavsson, Q. X. Zhao, M. Sadeghi, and A. Larsson, "Growth of GaInNAs and 1.3 μm edge emitting lasers by molecular beam epitaxy," J. Cryst. Growth **311**, 1863–1867 (2009).
10. P. Carrier and S.-H. Wei, "Calculated spin-orbit splitting of all diamondlike and zinc-blende semiconductors: effects of $p_{1/2}$ local orbitals and chemical trends," Phys. Rev. B **70**, 035212 (2004).
11. B. Fluegel, S. Francoeur, A. Mascarenhas, S. Tixier, E. C. Young, and T. Tiedje, "Giant spin-orbit bowing in $GaAs_{1-x}Bi_x$," Phys. Rev. Lett. **97**, 067205 (2006).
12. L. Wang, L. Zhang, L. Yue, D. Liang, X. Chen, Y. Li, P. Lu, J. Shao, and S. Wang, "Novel dilute bismide, epitaxy, physical properties and device application," Crystals **7**, 63 (2017).
13. M. C. Y. Huang, Y. Zhou, and C. J. Chang-Hasnain, "A nanoelectromechanical tunable laser," Nat. Photonics **2**, 180–184 (2008).
14. C.-Z. Ning, L. Dou, and P. Yang, "Bandgap engineering in semiconductor alloy nanomaterials with widely tunable compositions," Nat. Rev. Mater. **2**, 17070 (2017).
15. M. T. Hill and M. C. Gather, "Advances in small lasers," Nat. Photonics **8**, 908–918 (2014).
16. S. H. Pan, S. S. Deka, A. E. Amili, Q. Gu, and Y. Fainman, "Nanolasers: second-order intensity correlation, direct modulation and electromagnetic isolation in array architectures," Prog. Quantum Electron. **59**, 1–18 (2018).
17. K. J. Vahala, "Optical microcavities," Nature **424**, 839–846 (2003).
18. N. H. Zhu, Z. Shi, Z. K. Zhang, Y. M. Zhang, C. W. Zou, Z. P. Zhao, Y. Liu, W. Li, and M. Li, "Directly modulated semiconductor lasers," IEEE J. Sel. Top. Quantum Electron. **24**, 1–19 (2018).
19. Z. Batool, S. Chatterjee, A. Chernikov, A. Duzik, R. Fritz, C. Gogineni, K. Hild, T. J. C. Hosea, S. Imhof, S. R. Johnson, Z. Jiang, S. Jin, M. Koch, S. W. Koch, K. Kolata, R. B. Lewis, X. Lu, M. Masnadi-Shirazi, J. M. Millunchick, P. M. Mooney, N. A. Riordan, O. Rubel, S. J. Sweeney, J. C. Thomas, A. Thränhardt, T. Tiedje, and K. Volz, "Bismuth-containing III–V semiconductors," in *Molecular Beam Epitaxy* (Elsevier, 2013), pp. 139–158.
20. F. Hao, P. Nordlander, M. T. Burnett, and S. A. Maier, "Enhanced tunability and linewidth sharpening of plasmon resonances in hybridized metallic ring/disk nanocavities," Phys. Rev. B **76**, 245417 (2007).
21. C. L. Yu, H. Kim, N. de Leon, I. W. Frank, J. T. Robinson, M. McCutcheon, M. Liu, M. D. Lukin, M. Loncar, and H. Park, "Stretchable photonic crystal cavity with wide frequency tunability," Nano Lett. **13**, 248–252 (2013).
22. X. Wu, W. Pan, Z. Zhang, Y. Li, C. Cao, J. Liu, L. Zhang, Y. Song, H. Ou, and S. Wang, "1.142 μm GaAsBi/GaAs quantum well lasers grown by molecular beam epitaxy," ACS Photon. **4**, 1322–1326 (2017).
23. S. Francoeur, S. A. Nikishin, C. Jin, Y. Qiu, and H. Temkin, "Excitons bound to nitrogen clusters in GaAsN," Appl. Phys. Lett. **75**, 1538–1540 (1999).
24. V. V. Chaldyshev, A. L. Kolesnikova, N. A. Bert, and A. E. Romanov, "Investigation of dislocation loops associated with AsSb nanoclusters in GaAs," J. Appl. Phys. **97**, 024309 (2005).
25. D. F. Reyes, J. M. Ulloa, A. Guzman, A. Hierro, D. L. Sales, R. Beanland, A. M. Sanchez, and D. González, "Effect of annealing in the Sb and In distribution of type II GaAsSb capped InAs quantum dots," Semicond. Sci. Technol. **30**, 114006 (2015).
26. Z. Zhang, L. Yang, V. Liu, T. Hong, K. Vahala, and A. Scherer, "Visible submicron microdisk lasers," Appl. Phys. Lett. **90**, 111119 (2007).
27. T. Zhou, J. Zhou, Y. Cui, X. Liu, J. Li, K. He, X. Fang, and Z. Zhang, "Microscale local strain gauges based on visible micro-disk lasers embedded in a flexible substrate," Opt. Express **26**, 16797–16804 (2018).
28. T. Zhou, X. Liu, Y. Cui, Y. Cheng, X. Fang, W. Zhang, B. Xiang, and Z. Zhang, "Cantilever-based microring lasers embedded in a deformable substrate for local strain gauges," AIP Adv. **8**, 075306 (2018).
29. K. Yamashita, M. Yoshimoto, and K. Oe, "Temperature-insensitive refractive index of GaAsBi alloy for laser diode in WDM optical communication," Phys. Status Solidi C **3**, 693–696 (2006).
30. Q. Gu and Y. Fainman, *Semiconductor Nanolasers* (Cambridge University, 2017).
31. S. L. Chuang, *Physics of Photonic Devices*, 2nd ed. (Wiley, 2009).
32. B. E. A. Saleh, *Fundamentals of Photonics*, 2nd ed. (Wiley, 2007).
33. Y. Tominaga, K. Oe, and M. Yoshimoto, "Low temperature dependence of oscillation wavelength in $GaAs_{1-x}Bi_x$ laser by photo-pumping," Appl. Phys. Express **3**, 062201 (2010).
34. T. Fuyuki, R. Yoshioka, K. Yoshida, and M. Yoshimoto, "Long-wavelength emission in photo-pumped $GaAs_{1-x}Bi_x$ laser with low temperature dependence of lasing wavelength," Appl. Phys. Lett. **103**, 202105 (2013).

35. P. Ludewig, N. Knaub, N. Hossain, S. Reinhard, L. Nattermann, I. P. Marko, S. R. Jin, K. Hild, S. Chatterjee, W. Stolz, S. J. Sweeney, and K. Volz, "Electrical injection Ga(AsBi)/(AlGa)As single quantum well laser," Appl. Phys. Lett. **102**, 242115 (2013).
36. R. Butkutė, A. Geizutis, V. Paccebutas, B. Cechaviccius, V. Bukauskas, R. Kundrotas, P. Ludewig, K. Volz, and A. Krotkus, "Multi-quantum well Ga(AsBi)/GaAs laser diodes with more than 6% of bismuth," Electron. Lett. **50**, 1155–1157 (2014).
37. T. Fuyuki, K. Yoshida, R. Yoshioka, and M. Yoshimoto, "Electrically pumped room-temperature operation of $GaAs_{1-x}Bi_x$ laser diodes with low-temperature dependence of oscillation wavelength," Appl. Phys. Express **7**, 082101 (2014).
38. H. Kim, Y. Guan, S. E. Babcock, T. F. Kuech, and L. J. Mawst, "Characteristics of OMVPE grown GaAsBi QW lasers and impact of post-growth thermal annealing," J. Appl. Phys. **123**, 113102 (2018).